Involvement of chondroitin sulfate E in the liver tumor focal formation of murine osteosarcoma cells

Key words: chondroitin sulfate/glycosaminoglycan/tumor/osteosarcoma/sulfation

Running title: Cell surface chondroitin sulfate in liver tumor focal formation.

Basappa[1,6,*], Sengottuvelan Murugan[1,*], Kazuki N. Sugahara[2,3], Chun Man Lee[2,4], Gerdy B. ten Dam[5], Toin H. van Kuppevelt[5], Masayuki Miyasaka[2], Shuhei Yamada[1,†], and Kazuyuki Sugahara[1,†]

[1]Graduate School of Life Science, Hokkaido University, Sapporo, Japan; [2]Laboratory of Immunodynamics, Department of Microbiology and Immunology, Osaka University, Graduate School of Medicine, Suita, Japan; [3]Vascular Mapping Center, Burnham Institute for Medical Research UCSB, University of California, Santa Barbara, CA; [4]Medical Center for Translational Research, Osaka University Hospital, Suita, Japan; [5]Department of Biochemistry, Nijmegen Centre for Molecular Life Sciences, Radboud University Nijmegen Medical Centre, Nijmegen, The Netherlands; and [6]Department of Chemistry, Bangalore University, Bangalore, India.

*Equal Contribution

[†]To whom correspondence may be addressed: Tel.: 81-(11)-706-9055; Fax: 81-(11)-706-9055; E-mail: tjohej@sci.hokudai.ac.jp

[†]To whom correspondence may be addressed: Tel.: 81-(11)-706-9054; Fax: 81-(11)-706-9056; E-mail: k-sugar@sci.hokudai.ac.jp

Abstract

Cell surface heparan sulfate plays a critical role in regulating the metastatic behavior of tumor cells, whereas the role of chondroitin sulfate/dermatan sulfate (CS/DS) has been little understood in this context. Here, we characterized CS/DS chains from the murine osteosarcoma cell line LM8G7, which forms tumor nodules in liver. Structural analysis of the CS/DS chains showed a higher proportion of GlcUAβ1-3GalNAc(4,6-*O*-disulfate) (E-units) in LM8G7 (12%) than in its parental cell line LM8 (6%), which rarely forms tumors in the liver. Immunostaining with GD3G7, an antibody specific to E-units, confirmed the higher expression of the epitope in LM8G7 than LM8 cells. The tumor focal formation of LM8G7 cells to the liver in mice was effectively inhibited by the pre-administration of CS-E (rich in E-unit) or the pre-incubation of the antibody GD3G7 with the tumor cells. CS-E or GD3G7 inhibited the adhesion of LM8G7 cells to a laminin-coated plate *in vitro*. In addition, the invasive ability of LM8G7 cells *in vitro* was also reduced by the addition of CS-E or the antibody. Further, CS-E or the antibody inhibited the proliferation of LM8G7 cells dose-dependently. The binding of LM8G7 cells to VEGF *in vitro* was also significantly reduced by CS-E and GD3G7. Thus, the present study reveals the significance of highly sulfated CS/DS structures in the liver colonization of osteosarcoma cells and also provides a framework for the development of GAG-based anti-cancer molecules.

Introduction

The metastatic cascade consists of various interactions between tumor cells and the host cells or components of the extracellular matrix (ECM) and involves migration, adhesion, and invasion, which are mediated by cell surface molecules (Fidler 2003). Proteoglycans (PGs), a class of cell surface adhesion molecules composed of glycosaminoglycan (GAG) side chains attached to core proteins, are expressed in the ECM, and have diverse functions including roles in growth factor-binding, cell-ECM interactions, cell-cell adhesion, cell proliferation, differentiation, tissue morphogenesis and embryogenesis (Liotta 1986; Esko and Selleck 2002). Heparan sulfate (HS) or chondroitin sulfate (CS)/dermatan sulfate (DS) side chains modulate the interaction of tumor cells with host cells and ECM components (Gallagher 1989; Iida et al. 1996), and play a critical role in regulating tumor initiation, progression, and metastasis (Sanderson 2001; Munesue et al. 2007).

The GAGs in normal tissues differ in quantity and type from those found during embryonic development and in tumors (Dietrich 1984). It has become increasingly clear that heterogeneity in the structure of HS is important in regulating disease processes including cancer (Nakanishi et al. 1992). Elevated levels of CS have also been reported in transformed cells (Lv et al. 2007). Alterations in CS structure in tumors have been correlated with an increase in malignancy (Iida et al. 1998). In animal experiments, chondroitinase (CSase) treatment slowed the progression of cancer, leading to the suggestion that CS-PGs on the surface of cancer cells are useful therapeutic targets (Denholm et al. 2001).

In addition to ECM components, malignant cells produce a variety of soluble factors such as tumor necrosis factor-α, vascular epidermal growth factor (VEGF), and heparin-binding epidermal growth factor-like growth factor (HB-EGF), which play a major role in tumor progression (Jayne et al. 2000). Among these, VEGF and its receptors, VEGFR-1 and VEGFR-2, are more highly expressed in a metastatic model than in non-metastatic neoplasms

and directly correlate with the extent of neovascularization and degree of proliferation (Takahashi et al. 1995). Generally it is assumed that these growth factors and other signaling proteins drive the oncogenic process through direct/indirect interactions with cell surface molecules.

Cell surface molecules such as HS regulate the signal transduction of tumor cells by interacting with various growth factors such as fibroblast growth factor-2 (FGF-2) (Mundhenke et al. 2002), VEGF (Iozzo et al. 2001), and HB-EGF (Chu et al. 2005). Likewise, a rare highly sulfated GlcUAβ1–3GalNAc(4S,6S) structure (the E-unit) in CS/DS chains, where 4S and 6S stand for 4-*O*- and 6-*O*-sulfate, respectively, plays an important role in the interaction of various functional proteins (growth factors/cytokines) (Deepa et al. 2002). In addition, the involvement of E-units in various biological functions such as neurite outgrowth (Sugahara et al. 2007)**,** bone formation and biomineralization has been reported (Miyazaki et al. 2008). However, the involvement of highly sulfated structures of CS/DS chains in the process of tumor formation in different organ sites is not well understood.

Recently, we reported the involvement of CS structures containing E-units in the metastasis of a Lewis lung carcinoma cell line (Li et al. 2008). An analysis of liver-specific tumor phenotypes has revealed the overexpression or specific structural changes of HS chains to be critical to the metastatic potential of melanoma cells (Tovari et al. 1997). These findings prompted us to examine whether structural differences in the CS/DS chains of osteosarcoma cells explain the metastatic potential. In the present study, we demonstrated that the E-unit-containing structure of CS/DS chains in murine osteosarcoma LM8G7 cells is involved in the liver tumor focal formation.

Results

Comparison of CS/DS Chains between LM8 and LM8G7 Cells

The amount and composition of the unsaturated disaccharides produced by digestion with CSase ABC from the CS/DS polysaccharide chains, which had been extracted from LM8 and LM8G7 cells, are tabulated in Table 1, and the representative anion-exchange HPLC chromatograms for the disaccharide analyses are shown in Fig. 1. The amounts of CS/DS in LM8G7 and LM8 cells were comparable. Upon digestion with CSase ABC, CS/DS chains from both the cell lines yielded $\Delta^{4,5}$HexUAα1–3GalNAc (ΔO-unit), $\Delta^{4,5}$HexUAα1–3GalNAc(6S) (ΔC-unit), $\Delta^{4,5}$HexUAα1–3GalNAc(4S) (ΔA-unit) and $\Delta^{4,5}$HexUAα1–3GalNAc(4S,6S) (ΔE-unit) in varying proportions. The degree of sulfation of CS/DS chains was relatively higher (0.55) in LM8G7 cells than in LM8 cells (0.41) (Table 1). The proportion of the highly sulfated disaccharide ΔE-unit was higher in LM8G7 cells (12%) than LM8 cells (6%). The proportion of ΔC-units was significantly lower in LM8G7 cells (9%) than in LM8 cells (13%), whereas the proportion of ΔA-units was higher in LM8G7 cells (24%) than LM8 cells (16%).

In view of the recent finding of a higher proportion of E-units in the highly metastatic Lewis lung carcinoma cell line LM66-H11 than in the low metastatic cell line P29 (Li et al. 2008), it was speculated that the higher proportion of E-units in the CS/DS preparation of LM8G7 cells may be a key factor in the tumor focal formation to the liver. To confirm the overexpression of E-units on the surface of LM8G7 cells, a phage display antibody (GD3G7) specific to CS-E (Li et al. 2008; ten Dam et al. 2007; Purushothaman et al. 2007) was used for the immunostaining of the osteosarcoma cell lines. LM8G7 cells were more strongly stained by GD3G7 than were LM8 cells (Fig. 2), suggesting higher levels of the expression of the E-unit.

Characterization of Anti-tumor Activity of CS Isoforms

To examine the involvement of CS/DS in the liver tumor focal formation, various commercial CS preparations such as CS-A, CS-C, and CS-E (100 μg) were individually pre-

injected into mice 30 min before the intravenous injection of LM8G7 cells. Among the CS preparations tested, CS-E characterized by a high proportion (62%) of E-units (Kinoshita et al. 1997), completely inhibited the colonization of LM8G7 cells (Fig. 3D), suggesting the importance of the E-unit in the tumor focal formation to the liver. Dose-dependent inhibition experiments showed that CS-E inhibited the tumor focal formation of LM8G7 cells strongly at 100 or 150 μg but not at all at low-doses (25 or 50 μg) (Fig. 4A). Heparin, a well-known anti-tumor agent (Borsig et al. 2001), also inhibited the liver colonization of LM8G7 cells (Fig. 3G), whereas CS-A or CS-C failed to inhibit it (Fig. 3B and Fig. 3C).

Anti-tumor Activity of the Antibody GD3G7

The higher expression of E-units on the surface of LM8G7 cells and the strong anti-tumor activity of CS-E led us to hypothesize that E-unit-containing CS/DS chains on the tumor cell surface are involved in the liver tumor focal formation. It should be noted that the colonization of LM8G7 cells is specific to the liver, and no tumor colony formation was observed in other mouse organs including the lungs (data not shown). To test our hypothesis, the antibody GD3G7, which recognizes E-unit-containing CS/DS chains, was used for anti-tumor assays. The pre-incubation of LM8G7 cells with the antibody (0.2 to 2 μg) for 30 min strongly inhibited the liver tumor focal formation in a dose-dependent manner (Fig. 3E and Fig. 4B), whereas the irrelevant antibody MPB49V (2 μg) failed to inhibit it (Fig. 3F and Fig. 3G), suggesting that the epitopes for the antibody GD3G7 play a key role in the liver colonization of LM8G7 cells.

Effects of CS-E and GD3G7 on Adhesion and Invasion of LM8G7 Cells

Effects of CS-A, CS-E (50 μg), or the antibody GD3G7 (2 μg) on the adhesion of LM8G7 cells to a laminin-coated plate were examined. Laminin, a major basement membrane protein, plays an important role in the interaction of tumor cells with the basement membrane during the extravasation step of metastasis (Baba et al. 2008). CS-E and the antibody GD3G7

inhibited the adhesion of LM8G7 cells to the substrate (Fig. 5). In contrast, CS-A or the control antibody MPB49V had no effect on the attachment of LM8G7 cells to laminin.

Since the adhesion of tumor cells to basement membranes is an initial step in the invasion process, it was examined whether the anti-tumor effects of CS-E and GD3G7 are also due to the inhibition of cell invasion. The effects of CS-A, CS-C, CS-E (50 μg), or GD3G7 (2 μg) on the invasion by LM8G7 cells of Matrigel^{TM} were tested. The invasive ability of the cells was reduced by CS-E and the antibody, but CS-A and CS-C had no significant effect (Fig. 6). These results indicate CS-E-like epitopes to be involved in the invasion by LM8G7 cells as well.

Effects of CS-E and the Antibody GD3G7 on the Proliferation of LM8G7 Cells

To examine the effects of GAGs and GD3G7 on cell proliferation, LM8G7 cells (5 x 10^3) were seeded and CS-A (100 μg), CS-C (100 μg), CS-E (50 to 150 μg), heparin (100 μg) or the antibody (2 to 5μg) in DMEM containing 10% FBS was added. CS-E and GD3G7 inhibited the proliferation in a dose-dependent manner (Fig. 7), whereas CS-A and CS-C showed no effect. Heparin, as a positive control, inhibited the proliferation of LM8G7 cells. These observations led us to conclude that CS/DS chains at the cell surface play a major role in the proliferation of tumor cells.

Comparison of the Binding of LM8G7 Cells to Various Growth Factors

VEGF, expressed by tumor cells, facilitates the progression of cancer (Asai et al. 1998). We examined the ability of LM8G7 cells to bind growth factors *in vitro*. LM8G7 cells interacted well with VEGF, FGF-2, midkine (MK) and hepatocyte growth factor (HGF), but the degree of binding was the greatest with VEGF (Fig. 8A). The attachment of LM8G7 cells to VEGF was strongly inhibited by addition of CS-E or the antibody GD3G7 but not inhibited by CS-A or CS-C. Heparin, a positive control, also inhibited the attachment of LM8G7 cells to VEGF (Fig. 8B).

Discussion

PGs associated with the surface of cancer cells have been recognized as important in a variety of cancers (Blackhall et al. 2001). Alterations in the level of expression of GAG structure and/or density on PGs can potentially make cancer cells highly versatile in modulating their behavior. For instance, significant changes in PG content and GAG structure in tumors have been reported (Theocharis et al. 2002). It has been demonstrated that the disaccharide composition of cell surface HS varies during the transition from human colon adenoma to carcinoma (Jayson et al. 1998). Low-sulfated HS facilitates metastasis through the adhesion of hepatoma cells to the ECM (Robinson et al. 1984). In addition, low levels of cell surface HS are correlated well with the high metastatic activity of many tumors (Sugahara et al. 1989; Redini et al. 1986; Kure et al. 1987; Timar et al. 1992).

This study revealed heterogeneous yet unique structures in the CS/DS chains of LM8 and LM8G7 cells. The major disaccharide present in LM8 and LM8G7 cells was the unsulfated unit, levels of which were lower in LM8G7 than LM8 cells. An important finding of this study was the higher proportion of E-units in the CS/DS chains of LM8G7 than LM8 cells. In addition, LM8G7 cells were more strongly immunostained by the antibody GD3G7 than were LM8 cells, supporting the increased expression of E-units in LM8G7 cells. The results of our study indicate the correlation between highly sulfated CS structures and the metastatic potential of osteosarcoma cells. To investigate the relationship between the CS-E-like-structures and the liver tumor focal formation, various CS isoforms including CS-E were administered into mice to evaluate their effects against the colonization of LM8G7 cells. Animals pre-injected with CS-E had no tumor nodules in the liver, but the mice injected with other CS isoforms had tumor nodules, indicating the anti-tumor role of CS-E. In addition, the antibody GD3G7 completely inhibited the tumor forming activity of LM8G7 cells in the liver,

suggesting the involvement of the GD3G7 epitope containing E-units in the liver tumor focal formation of LM8G7 cells. These results are consistent with our recent finding that the experimental metastasis of the mouse Lewis lung carcinoma cell line involves the E-unit-containing epitope on the cell surface and is strongly inhibited by exogenous CS-E and the antibody GD3G7. It has also been reported that the epitope structure of GD3G7 is highly expressed in human ovarian carcinomas (ten Dam et al. 2007) and human pancreatic tumors (Sugahara et al. 2008). However, it remains to be established whether E-unit-containing structures are involved in the natural metastasis of human tumors. A high-throughput survey using tissue microarrays for the epitope of the antibody GD3G7 in natural human tumors (Sugahara et al. 2008) will clarify whether the epitope can be used as a tumor marker for diagnosis and is a therapeutic target of certain cancers.

Tumor formation in the distinct organs has been suggested to be essential for the development of metastasis. To investigate the mechanistic basis for the anti-tumor activity of CS-E against LM8G7 cells, we performed adhesion, invasion, and proliferation experiments *in vitro* to validate the effects of CS isoforms on the liver tumor focal formation of LM8G7 cells. We dynamically monitored the attachment of tumor cells to the laminin-coated plate in the presence or absence of CS isoforms or the antibody GD3G7. Both CS-E and GD3G7 markedly inhibited the attachment of LM8G7 cells to the laminin-coated plate. Therefore, it is reasonable to hypothesize that the pre-administration of CS-E may weakening tumor cell adhesion to endothelial cells thereby preventing the liver colonization. Further, the invasive ability of LM8G7 cells was significantly reduced by CS-E, but not by the other isoforms. Supporting this observation, GD3G7 also strongly inhibited the invasion by LM8G7 cells. Next, we tested the effects of CS-A, CS-C, CS-E or GD3G7 on cell proliferation. CS-E and GD3G7 inhibited the proliferation of LM8G7 cells in a dose-dependent manner. These results

suggest the E-unit-containing epitopes to be involved in the tumor forming process and a potential target for the diagnosis and treatment of osteosarcoma tumors.

It is well known that VEGF-releasing metastatic tumor cells dysregulate the endothelial cell-cell junctional complex upon binding and facilitates tumor extravasation (Weis et al. 2004). In this study, the addition of CS-E or GD3G7 strongly inhibited the interaction of tumor cells with VEGF. The most plausible explanation for this inhibition would be the direct binding of soluble CS-E to immobilized VEGF thereby preventing the attachment of tumor cells to VEGF, since it has been reported that highly sulfated CS-E interacts with VEGF *in vitro* (ten Dam et al. 2007). These results may also explain the inhibitory effects of CS-E on the liver colonization of LM8G7 cells. Thus, the present study reveals the significance of highly sulfated CS/DS structures in the liver tumor focal formation of the osteosarcoma cells and also provides a framework for the development of GAG-based anti-cancer molecules (Yamada and Sugahara 2008).

Materials and methods

Materials

Standard unsaturated CS disaccharides, CSase ABC (EC 4.2.2.4), CS-A from whale cartilage, CS-C from shark cartilage, and CS-E from squid cartilage and cell proliferation assay kit TetraColor One were purchased from Seikagaku Corp. (Tokyo, Japan). Recombinant human (rh)-HGF was from PeproTech EC Ltd (London, UK). rh-VEGF-165, rh-FGF-2, and rh-MK were obtained from Wako Pure Chemicals Co. (Osaka, Japan). The single chain antibody GD3G7 was selected for reactivity with rat embryo-derived GAGs by the phage display technique (ten Dam et al. 2007). The monoclonal anti-vesicular stomatitis virus glycoprotein (VSV-G) tag antibody P5D4 was from Sigma. Porcine intestinal mucosal heparin was obtained from Nacalai Tesque (Kyoto, Japan). Alexa Fluor 488-conjugated goat anti-mouse

IgG (H+L) was obtained from Invitrogen. Actinase E was from Kaken Pharmaceutical Co. (Tokyo, Japan). Mouse sarcoma laminin from basement membrane of Engelbreth-Holm Swarm was obtained from Sigma. 2-Aminobenzamide (2AB) was purchased from Nacalai Tesque (Kyoto, Japan). Sodium cyanoborohydride ($NaBH_3CN$) was from Aldrich Chemical Co. (Milwaukee, WI). 100X non-essential amino acids, β-mercaptoethanol, 100X sodium pyruvate, the cell dissociation buffer, and L-glutamine were from GIBCO (Auckland, New Zealand). Diff-Quick solution was from International Reagent Corp. (Kobe, Japan). All other chemicals and reagents were of the highest quality available.

Animals and Cell Lines

Nine-week-old female C3H/HeN mice were obtained from Japan SLC (Hamamatsu, Japan) and kept in standard housing. All the experiments were performed according to protocols approved by the local animal care committee of Hokkaido University. The murine osteosarcoma cell line LM8G7, which has high metastatic potential to liver, was cloned from LM8G5 cells (Lee et al. 2002) as described (Fidler and Nicolson 1976) and cultured in DMEM supplemented with 10% (v/v) FBS (Thermo Trace, Melbourne, Australia), streptomycin (100 μg/ml), penicillin (100 units/ml), 100X non-essential amino acids, β-mercaptoethanol (50 μM), 100X sodium pyruvate, and L-glutamine (2 mM) at 37 °C in a humidified 5% CO_2 atmosphere. The cells were harvested after being incubated with 0.1% trypsin/1 mM EDTA in phosphate-buffered saline (PBS) for 5 min at 37 °C, gently flushed with a pipette, and subcultured three times a week.

Extraction of GAGs from LM8 and LM8G7 Cells

Cells were dehydrated and delipidated by extraction with acetone, air-dried and used for the extraction of GAGs essentially as described previously (Li et al. 2007) with some modifications. Briefly, the acetone powder was digested with heat-activated (60 °C, 30 min) actinase E in 200 μl of 0.1 M sodium borate, pH 8.0, containing 10 mM calcium acetate at

60 °C for 48 h. After the incubation, each sample was treated with 5% trichloroacetic acid and kept for 30 min at 4 °C. The precipitate was removed by centrifugation. The supernatant was extracted with diethyl ether to remove the trichloroacetic acid. After neutralization with 1.0 M sodium carbonate, the aqueous phase was adjusted to contain 80% ethanol and 1% sodium acetate, and kept at 4 °C overnight. The precipitated crude GAGs were recovered by centrifugation, desalted on a PD-10 column (GE Healthcare) using 50 mM pyridine acetate buffer, pH 5.0, as an eluent, and evaporated dry.

Analysis of the Disaccharide Composition of CS Chains

The disaccharide composition of GAG preparations from the osteosarcoma cell lines was determined as described (Li et al. 2007). Briefly, the samples were dissolved in water and an aliquot was digested with CSase ABC (Saito et al. 1968), and labeled with 2AB (Kinoshita et al. 1999). The excess 2AB was removed by extraction with chloroform (Kawashima et al. 2002). The 2AB-labeled digest was analyzed by anion-exchange HPLC on a PA-03 silica column (YMC-Pack PA, Kyoto, Japan) with a linear gradient of NaH_2PO_4 from 16 to 538 mM over 60 min at a flow rate of 1.0 ml/min at room temperature. Identification and quantification of the resulting disaccharides were achieved by comparison with the elution of authentic CS-derived unsaturated disaccharides (Kinoshita et al. 1999).

Immunocytochemistry

To detect the E-unit-containing epitopes, murine osteosarcoma cell lines, LM8 and LM8G7, were stained using a phage display single chain antibody, GD3G7 (ten Dam et al. 2007; Purushothaman et al. 2007). Briefly, osteosarcoma cells were plated on 8-well Lab-Tech chamber slides (Nalge Nunc International), cultured for 24 h, and fixed with Diff-Quick reagent A. After being blocked with PBS containing 3% bovine serum albumin (BSA) for 1 h at room temperature, the fixed cells were incubated with 100 μl of the primary antibody GD3G7 (diluted 1:100 (10 μg/ml) in 0.1% BSA/PBS) for 1 h at room temperature, and

washed with PBS. After being incubated with the anti-VSV-G antibody (diluted 1:5,000 in 0.1% BSA/PBS) for 1 h at room temperature, the cells were washed with PBS. To detect the anti-VSV-G antibody, the cells were stained with a third antibody conjugated to Alexa Fluor 488 (diluted 1:500 in 0.1% BSA/PBS), and visualized with a laser-scanning confocal microscope, FLUOVIEW (Olympus, Tokyo, Japan).

Assay of Liver Tumor Focal Formation

In preparation for injection, LM8G7 cells were harvested after a brief exposure to a cell dissociation buffer (GIBCO) and the cell viability in single-cell suspensions was determined by trypan blue exclusion. A total of 1 x 10^6 cells suspended in 200 μl of DMEM were injected into a lateral tail vein of C3H/HeN mice. Four weeks later, the animals were sacrificed. The number of visible tumor cell nodules in the liver was examined and liver weight was recorded.

To elucidate the involvement of cell surface CS/DS in the liver tumor focal formation, the C3H/HeN mice received 100 μg of commercial CS preparations (CS-A, CS-C, or CS-E) or heparin 30 min before the tumor cell injection. The dose-dependent inhibition experiments were carried out using CS-E (25, 50, 100, or 150 μg). In other instances, to investigate the involvement of the antibody GD3G7 epitope in the liver tumor focal formation, LM8G7 cells were pre-incubated with serially diluted GD3G7 (0.05, 0.1, 0.2, 0.5, 1, or 2 μg) or the irrelevant antibody MPB49V (2 μg) for 30 min at 37 °C. Aliquots of the cell suspension were assessed for cell viability before the injection. After incubated with antibodies (GD3G7 or MPB49V) and prior to the injection of the tumor cells into animals, it was ensured by microscopic observations that these cells were in a single cell suspension.

Real-Time Monitoring of the Adhesion of LM8G7 Cells to the Laminin Substrate

The cell attachment assay was carried out using RT-CES™ system (ACEA Biosciences, San Diego, CA). ACEA's 96X microtiter plates were coated with laminin (0.5 μg/well) at 37 °C

for 1 h. Attachment and spreading of LM8G7 cells (2 x 10^4) were monitored in the presence or absence of various inhibitors such as CS-A (50 μg), CS-E (50 μg), the antibody GD3G7 (2 μg), or the control antibody MPB49V (2 μg), and continuously monitored for up to 62 min using the RT-CES™ system. The cell index (quantitative measurement of cells in a well containing an electrode) was plotted against time.

Cell Invasion Assay In Vitro

The invasion of LM8G7 cells across the Matrigel™-coated porous membranes was assessed using a 24-well plate (8 μm pore size, insert size: 6.4 μm) (BD Biosciences) according to the manufacturer's protocol. Briefly, single cell suspensions of LM8G7 cells (2.5 x 10^4) were prepared by detaching and resuspending the cells in DMEM containing 0.1% BSA. Before the cells were added, the chambers were rehydrated for 2 h in an incubator at 37 °C. The lower chambers were filled with DMEM containing 5% FBS. In some instances, LM8G7 cells (2.5 x 10^4) in serum-free DMEM were pre-incubated with CS-A, CS-C, CS-E (50 μg) or the antibody GD3G7 (2 μg) for 30 min at 37 °C in a CO_2 incubator, and added to the upper chamber. After incubation for 24 h, cells that had passed through the Matrigel-coated membrane and remained attached to the opposite surface of the membrane were stained with the Diff-Quick solution, and counted in five random microscopic fields per filter.

Assay of Cell Proliferation In Vitro

To examine the effects of CS isoforms on proliferation *in vitro*, LM8G7 cells were seeded at a density of 5 x 10^3 cells/well in a 96-well plate and treated with CS-E (50 to 150 μg), GD3G7 (2 to 5 μg), CS-A (100 μg), CS-C (100 μg) or heparin (100 μg) for 3 days. After a specific period of time, 5 μL of TetraColor One (Tanaka et al. 2002) reagent was added and incubated for an additional 4 h and the absorbance at 450 nm (Bio-Rad) was measured. The viability of the cells was expressed in percentage terms.

Tumor Cell-Growth Factor Adhesion Assay

The adhesion of tumor cells to various growth factors (Hibino et al. 2005) *in vitro* was assessed in a 96-well plate. VEGF, FGF-2, MK and HGF (100 ng) were added to the microtiter plate and incubated overnight at 4 °C. After blocking the wells with 1% BSA in PBS, DMEM containing LM8G7 cells (2.5 x 10^4) in 0.1% BSA were added to a plate and incubated for 1 h at 37 °C in a humidified 5% CO_2 atmosphere. After a brief wash with PBS, 100 μl of PBS containing 5 μl of TetraColor One was added and the plate was incubated for 45 min. The viable adhered cells were quantified by measuring the absorbance at 450 nm. The net signal is obtained by subtracting the background obtained with a BSA-coated well. In other instances, the cells were pre-incubated with CS-A, CS-C, CS-E, heparin (50 μg) or GD3G7 (2 μg) for 30 min at 37 °C and used for the experiment.

Funding

*This work was supported in part by a Grant-in-aid (20390019) from the Ministry of Education, Culture, Sports, Science, and Technology of Japan (MEXT), the New Energy and Industrial Technology Development Organization (NEDO) (to K. S.), the Human Frontier Science Program (RGP62/2004 to T.H.v.K.), the Dutch Cancer Society, grant number 2008-4058 (to G. t. D.). Basappa and Sengottuvelan Murugan are grateful to the Japan Society for the Promotion of Science (JSPS) for a postdoctoral fellowship

Abbreviations

Extracellular matrix, ECM; glycosaminoglycan, GAG; heparan sulfate, HS; chondroitin sulfate, CS; dermatan sulfate, DS; vascular epidermal growth factor, VEGF; fibroblast growth factor-2, FGF-2; hepatocyte growth factor, HGF; midkine, MK; 2-aminobenzamide, 2AB; Dulbecco's modified Eagle's medium, DMEM; fetal bovine serum, FBS; phosphate-buffered saline, PBS; bovine serum albumin, BSA; D-glucuronic acid, GlcUA; *N*-acetyl-D-

galacotosamine, GalNAc; 4-*O*-sulfate, 4S; 6-*O*-sulfate, 6S; GlcUAβ1–3GalNAc(4S,6S), E-unit; hexuronic acid, HexUA; 4,5-unsaturated hexuronic acid, $\Delta^{4,5}$HexUA.

References

Asai T, Ueda T, Itoh K, Yoshioka K, Aoki Y, Mori S, Yoshikawa H. 1998. Establishment and characterization of a murine osteosarcoma cell line (LM8) with high metastatic potential to the lung. *Int J Cancer.* 76:418-422.

Baba Y, Iyama KI, Hirashima K, Nagai Y, Yoshida N, Hayashi N, Miyanari N, Baba H. 2008. Laminin-332 promotes the invasion of oesophageal squamous cell carcinoma via PI3K activation. *Br J Cancer.* 98:974-980.

Blackhall FH, Merry CL, Davies EJ, Jayson GC. 2001. Heparan sulfate proteoglycans and cancer. *Br J Cancer.* 19:1094-1098.

Borsig L, Wong R, Feramisco J, Nadeau DR, Varki NM, Varki A. 2001. Heparin and cancer revisited: mechanistic connections involving platelets, P-selectin, carcinoma mucins, and tumor metastasis. *Proc Natl Acad Sci USA.* 98:3352-3357.

Chu CL, Goerges AL, Nugent MA. 2005. Identification of common and specific growth factor binding sites in heparan sulfate proteoglycans. *Biochemistry.* 44:12203-12213.

Denholm EM, Lin YQ, Silver PJ. 2001. Anti-tumor activities of chondroitinase AC and chondroitinase B: inhibition of angiogenesis, proliferation and invasion. *Eur J Pharmacol.* 416:213-221.

Deepa SS, Umehara Y, Higashiyama S, Itoh N, Sugahara K. 2002. Specific molecular interactions of oversulfated chondroitin sulfate E with various heparin-binding growth factors. Implications as a physiological binding partner in the brain and other tissues. *J Biol Chem.* 277:43707-43716.

Dietrich CP. 1984. A model for cell-cell recognition and control of cell growth mediated by sulfated glycosaminoglycans. *Braz J Med Biol Res.* 17:5-15.

Esko JD, Selleck SB. 2002. Order out of chaos: assembly of ligand binding sites in heparan sulfate. *Annu Rev Biochem.* 71:435-471.

Fidler IJ. 2003. The pathogenesis of cancer metastasis: the 'seed and soil' hypothesis revisited. *Nat Rev Cancer.* 3:453-458.

Fidler IJ, Nicolson GL. 1976. Organ selectivity for implantation survival and growth of B16 melanoma variant tumor lines. *J Natl Cancer Inst.* 57:1199-11202.

Gallagher JT. 1989. The extended family of proteoglycans: social residents of the pericellular zone. *Curr Opin Cell Biol.* 1:1201-1218.

Hibino S, Shibuya M, Hoffman MP, Engbring JA, Hossain R, Mochizuki M, Kudoh S, Nomizu M, Kleinman HK. 2005. Laminin alpha5 chain metastasis- and angiogenesis-inhibiting peptide blocks fibroblast growth factor 2 activity by binding to the heparan sulfate chains of CD44. *Cancer Res.* 65:10494-10501.

Iida J, Meijne AM, Knutson JR, Furcht LT, McCarthy JB. 1996. Cell surface chondroitin sulfate proteoglycans in tumor cell adhesion, motility and invasion. *Semin Cancer Biol.* 7:155-162.

Iida J, Meijne AM, Oegema TR Jr, Yednock TA, Kovach NL, Furcht LT, McCarthy JB. 1998. A role of chondroitin sulfate glycosaminoglycan binding site in alpha4beta1 integrin-mediated melanoma cell adhesion. *J Biol Chem.* 273:5955-5962.

Iozzo RV. 1998. Matrix proteoglycans: from molecular design to cellular function. *Annu Rev Biochem.* 67:609-652.

Iozzo RV, San Antonio JD. 2001. Heparan sulfate proteoglycans: heavy hitters in the angiogenesis arena. *J Clin Invest.* 108:349-55.

Kawashima H, Atarashi K, Hirose M, Hirose J, Yamada S, Sugahara K, Miyasaka M. 2002. Oversulfated chondroitin/dermatan sulfates containing GlcAbeta1/IdoAalpha1-3GalNAc(4,6-*O*-disulfate) interact with L- and P-selectin and chemokines. *J Biol Chem.* 277:12921-2930.

Kinoshita A, Sugahara K. 1999. Microanalysis of glycosaminoglycan-derived oligosaccharides labeled with a fluorophore 2-aminobenzamide by high-performance liquid chromatography: application to disaccharide composition analysis and exosequencing of oligosaccharides. *Anal Biochem.* 269:367-378.

Kinoshita A, Yamada S, Haslam SM, Morris HR, Dell A, Sugahara K. 1997. Novel tetrasaccharides isolated from squid cartilage chondroitin sulfate E contain unusual sulfated disaccharide units GlcA(3-*O*-sulfate)beta1-3GalNAc(6-*O*-sulfate) or GlcA(3-*O*-sulfate)beta1-3GalNAc. *J Biol Chem.* 272:19656-19665.

Kure S, Yoshie O, Aso H. 1987. Metastatic potential of murine B16 melanoma correlates with reduced surface heparan sulfate glycosaminoglycan. *Jpn J Cancer Res.* 78:1238-1245.

Jayne DG, Perry SL, Morrison E, Farmery SM, Guillou PJ. 2000. Activated mesothelial cells produce heparin-binding growth factors: implications for tumour metastases. *Br J Cancer.* 82:1233-1238.

Jayson GC, Lyon M, Paraskeva C, Turnbull JE, Deakin JA, Gallagher JT. 1998. Heparan sulfate undergoes specific structural changes during the progression from human colon adenoma to carcinoma in vitro. *J Biol Chem.* 273:51-57.

Lee CM, Tanaka T, Murai T, Kondo M, Kimura J, Su W, Kitagawa T, Ito T, Matsuda H, Miyasaka M. 2002. Novel chondroitin sulfate-binding cationic liposomes loaded with cisplatin efficiently suppress the local growth and liver metastasis of tumor cells in vivo. *Cancer Res.* 62:4282-4288.

Li F, Shetty AK, Sugahara K. 2007. Neuritogenic activity of chondroitin/dermatan sulfate hybrid chains of embryonic pig brain and their mimicry from shark liver. Involvement of the pleiotrophin and hepatocyte growth factor signaling pathways. *J Biol Chem.* 282:2956-2966.

Li F, ten Dam GB, Murugan S, Yamada S, Hashiguchi T, Mizumoto S, Oguri K, Okayama M, van Kuppevelt TH, Sugahara K. 2008. Involvement of highly sulfated chondroitin sulfate in the metastasis of the Lewis lung carcinoma cells. *J Biol Chem.* 283:34294-34304.

Liotta L.A. 1986. Tumor invasion and metastases-role of the extracellular matrix. *Cancer Res.* 46:1-7.

Lv H, Yu G, Sun L, Zhang Z, Zhao X, Chai W. 2007. Elevate level of glycosaminoglycans and altered sulfation pattern of chondroitin sulfate are associated with differentiation status and histological type of human primary hepatic carcinoma. *Oncology.* 72:347-356.

Miyazaki T, Miyauchi S, Tawada A, Anada T, Matsuzaka S, Suzuki O. 2008. Oversulfated chondroitin sulfate-E binds to BMP-4 and enhances osteoblast differentiation. *J Cell Physiol.* 217:769-777.

Mundhenke C, Meyer K, Drew S, Friedl A. 2002. Heparan sulfate proteoglycans as regulators of fibroblast growth factor-2 receptor binding in breast carcinomas. *Am J Pathol.* 160:185-94.

Munesue S, Yoshitomi Y, Kusano Y, Koyama Y, Nishiyama A, Nakanishi H, Miyazaki K, Ishimaru T, Miyaura S, Okayama M, Oguri K. 2007. A novel function of syndecan-2, suppression of matrix metalloproteinase-2 activation, which causes suppression of metastasis. *J Biol Chem.* 282:28164-28174.

Nakanishi H, Oguri K, Yoshida K, Itano N, Takenaga K, Kazama T, Yoshida A, Okayama M. Structural differences between heparan sulphates of proteoglycan involved in the formation of basement membranes in vivo by Lewis-lung-carcinoma-derived cloned cells with different metastatic potentials. 1992. *Biochem J.* 288:215-224.

Purushothaman A, Fukuda J, Mizumoto S, ten Dam GB, van Kuppevelt TH, Kitagawa H, Mikami T, Sugahara K. 2007. Functions of chondroitin sulfate/dermatan sulfate chains in brain development. Critical roles of E and iE disaccharide units recognized by a single

chain antibody GD3G7. *J Biol Chem.* 282:19442-19452.

Redini F, Moczar E, Poupon MF. 1986. Cell surface glycosaminoglycans of rat rhabdomyosarcoma lines with different metastatic potentials and of non-malignant rat myoblasts. *Biochim Biophys Acta.* 883:98-105.

Robinson J, Viti M, Höök M. 1984. Structure and properties of an under-sulfated heparan sulfate proteoglycan synthesized by a rat hepatoma cell line. *J Cell Biol.* 98:946-953.

Saito H, Yamagata T, Suzuki S. 1968. Enzymatic methods for the determination of small quantities of isomeric chondroitin sulfates. *J Biol Chem.* 243:1536-1542.

Sanderson RD. 2001. Heparan sulfate proteoglycans in invasion and metastasis. *Semin Cell Dev Biol.* 12:89-98.

Sugahara K, Mikami T. 2007. Chondroitin/dermatan sulfate in the central nervous system. *Curr Opin Struct Biol.* 17:536-545.

Sugahara K, Okumura Y, Yamashina I. 1989. The Engelbreth-Holm-Swarm mouse tumor produces undersulfated heparan sulfate and oversulfated galactosaminoglycans. *Biochem Biophys Res Commun.* 162:189-197.

Sugahara KN, Hirata T, Tanaka T, Ogino S, Takeda M, Terasawa H, Shimada I, Tamura J, ten Dam GB, van Kuppevelt TH, Miyasaka M. 2008. Chondroitin sulfate E fragments enhance CD44 cleavage and CD44-dependent motility in tumor cells. *Cancer Res.* 68:7191-7199.

Takahashi Y, Kitadai Y, Bucana CD, Cleary KR, Ellis LM. 1995. Expression of vascular endothelial growth factor and its receptor, KDR, correlates with vascularity, metastasis, and proliferation of human colon cancer. *Cancer Res.* 55:3964-3968.

Tanaka Y, Nakayamada S, Fujimoto H, Okada Y, Umehara H, Kataoka T, Minami Y. 2002. H-Ras/mitogen-activated protein kinase pathway inhibits integrin-mediated adhesion and induces apoptosis in osteoblasts. *J Biol Chem.* 277:21446-21452.

Theocharis AD. 2002. Human colon adenocarcinoma is associated with specific post-translational modifications of versican and decorin. *Biochim Biophys Acta.* 1588:165-172.

Timar J, Ladanyi A, Lapis K, Moczar M. 1992. Differential expression of proteoglycans on the surface of human melanoma cells characterized by altered experimental metastatic potential. *Am J Pathol.* 141:467-474.

ten Dam GB, van de Westerlo EM, Purushothaman A, Stan RV, Bulten J, Sweep FC, Massuger LF, Sugahara K, van Kuppevelt TH. 2007. Antibody GD3G7 selected against embryonic glycosaminoglycans defines chondroitin sulfate-E domains highly up-regulated in ovarian cancer and involved in vascular endothelial growth factor binding. *Am J Pathol.* 171:1324-1333.

Tóvári J, Paku S, Rásó E, Pogány G, Kovalszky I, Ladányi A, Lapis K, Tímár J. 1997. Role of sinusoidal heparan sulfate proteoglycan in liver metastasis formation. *Int J Cancer.* 71:825-831.

Weis S, Cui J, Barnes L, Cheresh D. 2004. Endothelial barrier disruption by VEGF-mediated Src activity potentiates tumor cell extravasation and metastasis. *J Cell Biol.* 167:223-229.

Yamada S, Sugahara K. 2008. Potential therapeutic application of chondroitin sulfate/dermatan sulfate. *Curr Drug Discov Technol.* 5:289-301.

Figure Legends

Fig. 1. Anion exchange HPLC of CSase ABC digests of the CS/DS chains obtained from the osteosarcoma cell lines LM8 and LM8G7. The CS/DS preparations were digested individually with CSase ABC. After 2AB-labeling, each digest was analyzed by HPLC on an amine-bound silica PA-03 column using a linear gradient of NaH_2PO_4 as indicated by the dashed line. The peaks before 10 min were derived from 2AB-derivatizing reagents. (A), authentic hyaluronan/CS-derived unsaturated disaccharides. (B) and (C), 2AB-labeled CS-derived unsaturated disaccharides obtained from LM8 and LM8G7 cells, respectively. Arrows indicate the elution positions of the 2AB-derivatized authentic hyaluronan and CS disaccharides: 1, $\Delta^{4,5}$HexUA-GlcNAc; 2, $\Delta^{4,5}$HexUA-GalNAc; 3, $\Delta^{4,5}$HexUA-GalNAc(6S); 4, $\Delta^{4,5}$HexUA-GalNAc(4S); 5, $\Delta^{4,5}$HexUA(2S)-GalNAc(6S); 6, $\Delta^{4,5}$HexUA-GalNAc(4S,6S); 7, ΔHexUA(2S)-GalNAc(4S, 6S).

Fig. 2. Immunocytological detection of the GD3G7 epitope on the surface of murine osteosarcoma LM8 and LM8G7 cells. LM8 (A) and LM8G7 (B) cells were seeded separately on chamber slides, cultured for 24 h, and fixed with Diff-Quick reagent A. They were incubated with the antibody GD3G7 for 1 h, and bound GD3G7 was detected with an anti-VSV glycoprotein antibody followed by an Alexa-conjugated third antibody, and visualized by confocal microscopy. In control experiments, LM8G7 cells were stained without GD3G7 (C) or irrelevant antibody MPB49V (D). Scale bar, 100 μm.

Fig. 3. Effects of CS isoforms and the antibody GD3G7 on the liver tumor focal formation of LM8G7 cells. The CS/DS preparation (100 μg) in 200 μl of Dulbecco's Modified Eagle's Medium (DMEM) was injected into a tail vein of C3H/HeN mouse 30 min before the injection of LM8G7 cells (1×10^6). LM8G7 cells were also pre-incubated with the antibody

GD3G7 (2 μg) or the control antibody MPB49V (2 μg) for 30 min at 37 ^{o}C and used for the tumor colonization experiments. Representative livers from the mice treated with DMEM (Control) (A), CS-A (B), CS-C (C), CS-E (D), antibody GD3G7 (E), or MPB49V (F) are shown. The average liver weight of the control and treated mice (G). Heparin from porcine intestinal mucosa (100 μg) was used as a positive control. The data represent mean values ± SD for two independent experiments. * $p < 0.01$ versus control. Mann-Whitney *U* test.

Fig. 4. Dose-dependent anti-tumor activity of CS-E and the antibody GD3G7. (A) The anti-tumor activity of various doses (25, 50, 100, or 150 μg) of CS-E was investigated as described in the legend to Fig. 2. (B) LM8G7 cells were pre-incubated with the antibody GD3G7 at different doses (0.05, 0.1, 0.2, 0.5, 1, or 2 μg) for 30 min, and used for the analysis of tumor focal formation as described in the legend to Fig. 2. Six mice were used per group. The data represent mean values ± SD for two independent experiments. * $p < 0.01$ versus control. Mann-Whitney *U* test.

Fig. 5. Real-time monitoring of the effects of CS-A, CS-E or GD3G7 on the adhesion of LM8G7 cells to the laminin substrate. LM8G7 cells (2 x 10^4) were seeded in ACEA's 96X e-plate™ coated with (Δ) or without laminin (◊) and the effects of CS-A (50 μg, ▲), CS-E (50 μg, o), GD3G7 (2 μg, ♦), and MPB49V (2 μg, □) were observed for 60 min using the RT-CES™ system as described in the *Materials and methods* section. The cell index (quantitative measurement of cells in a well containing an electrode) values were plotted against time. The data represent mean values ± SD for three independent experiments.

Fig. 6. Effects of various CS isoforms and the antibody GD3G7 on the invasion of LM8G7 cells. (A) The invasion of LM8G7 cells (2.5 x 10^4) was measured using a BD BioCoat™

chamber (BD Biosciences) coated with Matrigel^{TM} in the presence or absence of CS-A, CS-C, CS-E (50 μg) or GD3G7 (2 μg) in the upper chamber and allowed to invade through the Matrigel for 24 h. The cell invasion was measured as described in the *Materials and methods* section. The number of invaded cells is presented. The data represent mean values ± SD for two independent experiments. * $p < 0.01$ versus control. Mann-Whitney *U* test.

Fig. 7. Effects of various GAGs and the antibody GD3G7 on the proliferation of LM8G7 cells. (A) LM8G7 cells (5 x 10^3) were plated on 96-well plates in DMEM supplemented with 10% fetal bovine serum (FBS) in the presence or absence of CS-A (100 μg), CS-C (100 μg), CS-E (50 to 150 μg), heparin (100 μg), or the antibody GD3G7 (2 or 5 μg). The number of viable cells was determined 3 days after seeding. The data represent mean values ± SD for three independent experiments. * $p < 0.01$ versus control. ** $p < 0.05$ versus control. Mann-Whitney *U* test.

Fig. 8. The effects of various GAGs on the attachment of LM8G7 cells to VEGF. (A) LM8G7 cells (2.5 x 10^4) were seeded on growth factor-coated plates and the cells attached were quantified as described in the *Materials and methods* section. The net signal obtained for the LM8G7 cells adhered to VEGF is presented. (C) The effects of GAGs or GD3G7 on the attachment of LM8G7 cells to the immobilized VEGF. LM8G7 cells were pre-incubated with CS-A, CS-C, CS-E, heparin (50 μg) or GD3G7 (2 μg) for 30 min at 37 ^{o}C, and their effects on the adhesion of VEGF were measured. Values obtained with control wells not treated with GAGs are taken as 100%. * $p < 0.01$ versus control. Mann-Whitney *U* test.

Table 1. Disaccharide composition of CS/DS chains in osteosarcoma cell lines LM8 and LM8G7[a]

Unsaturated disaccharide	LM8	LM8G7
	pmol (mol %)	
ΔO: ΔHexUA-GalNAc	65.7 (64.9)	50.4 (55.8)
ΔC: ΔHexUA-GalNAc(6S)	13.0 (12.8)	7.4 (8.6)
ΔA: ΔHexUA-GalNAc(4S)	15.8 (15.8)	21.4 (23.7)
ΔD: ΔHexUA(2S)-GalNAc(6S)	N.D.[d]	N.D.
ΔB: ΔHexUA(2S)-GalNAc(4S)	N.D.	N.D.
ΔE: ΔHexUA-GalNAc(4S,6S)	6.6 (6.5)	10.7 (11.9)
ΔT: ΔHexUA(2S)-GalNAc(4S, 6S)	N.D.	N.D.
Total[b]	101.2 (100)	90.0 (100)
S/unit[c]	0.41	0.55
Molar ratio of the total disaccharides[e]	1.12 : 1.00	

[a]The GAG preparation from each osteosarcoma cell line was digested with CSase ABC and the digest was analyzed by anion-exchange HPLC after labeling with a fluorophore 2-AB as described in the *Materials and methods* section.

[b]Amounts of disaccharides/mg of dried cells.

[c]A molar ratio of sulfate to disaccharide.

[d]N.D., not detected.

[e]A molar ratio of the total CS/DS disaccharides of the two cell lines.

Fig 1

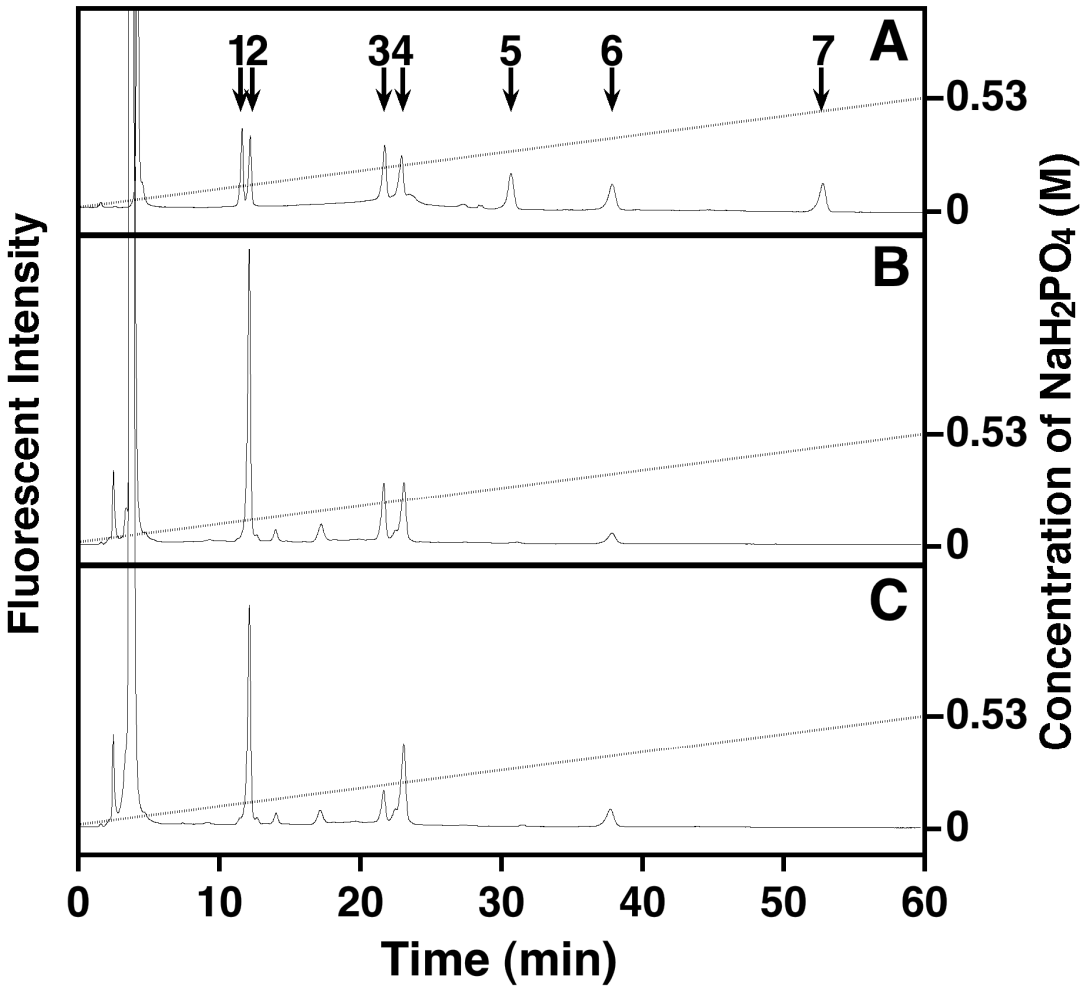
12
34
5
6
7
A
B
C
0.53
0
0.53
0
0.53
0
Fluorescent Intensity
Concentration of NaH2PO4 (M)
0
10
20
30
40
50
60
Time (min)

Fig 2

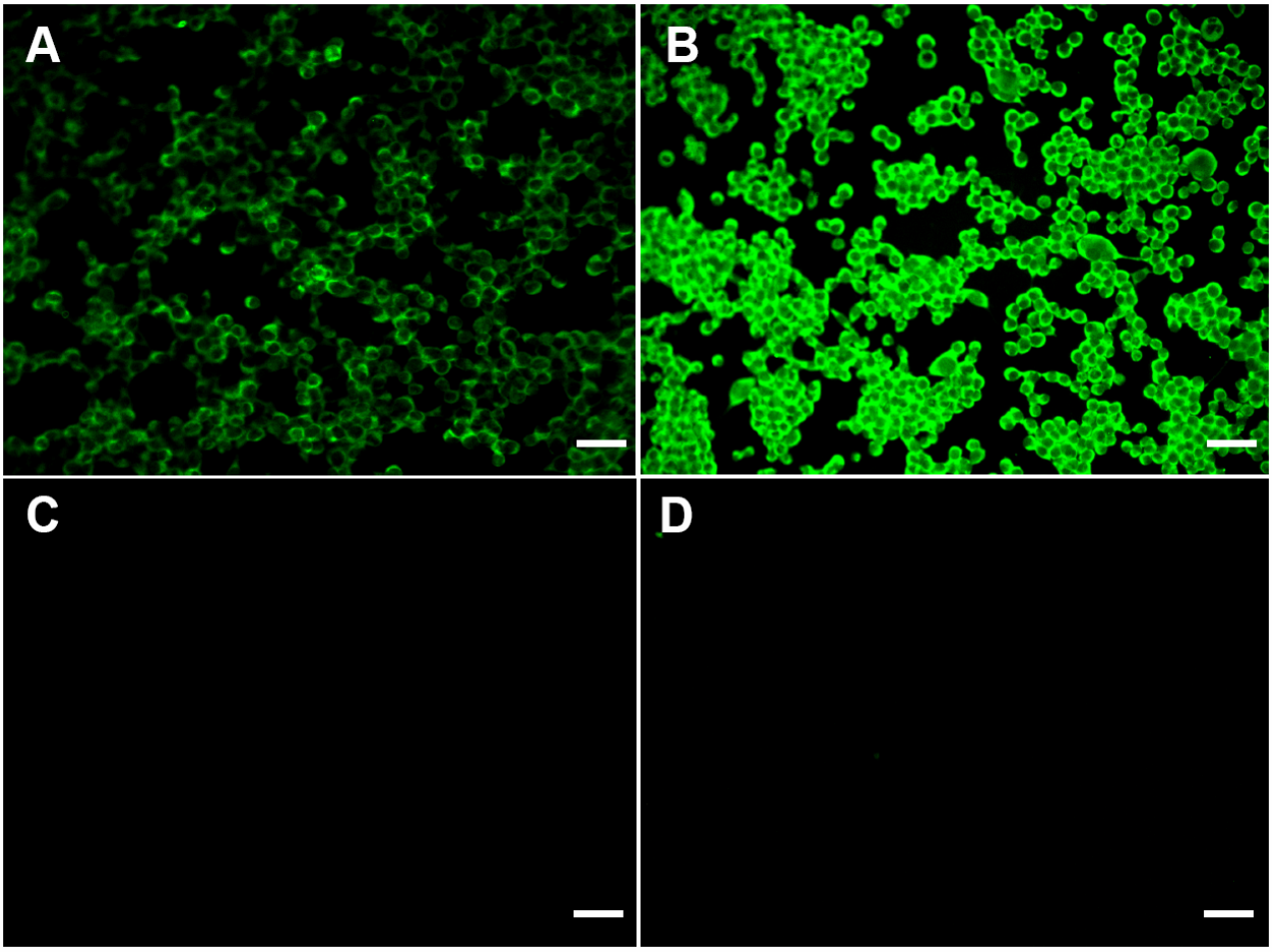

Fig 3

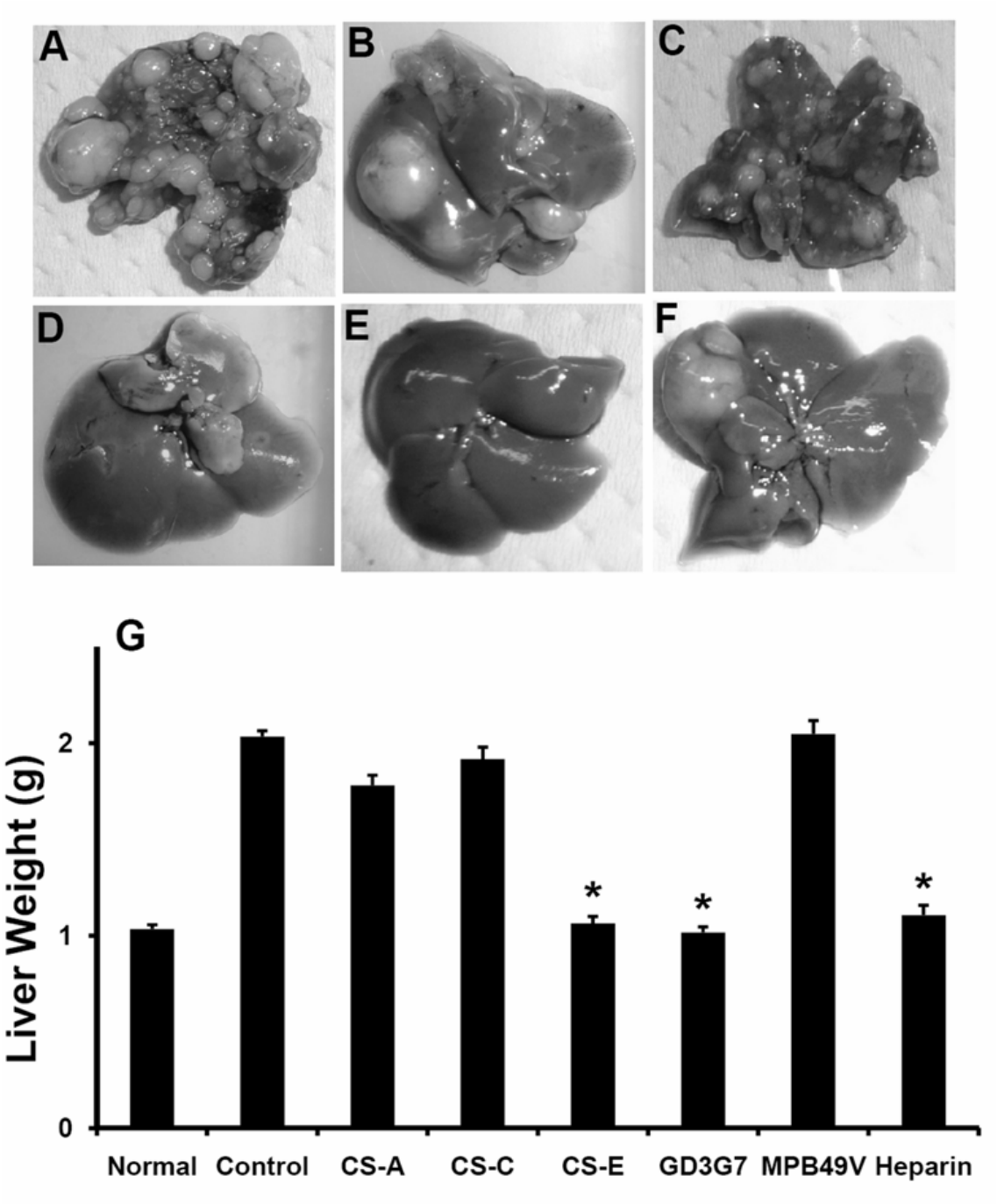
A
B
C
D
E
F
G
Liver Weight (g)
0
1
2
*
*
*
Normal
Control
CS-A
CS-C
CS-E
GD3G7
MPB49V
Heparin

Fig 4

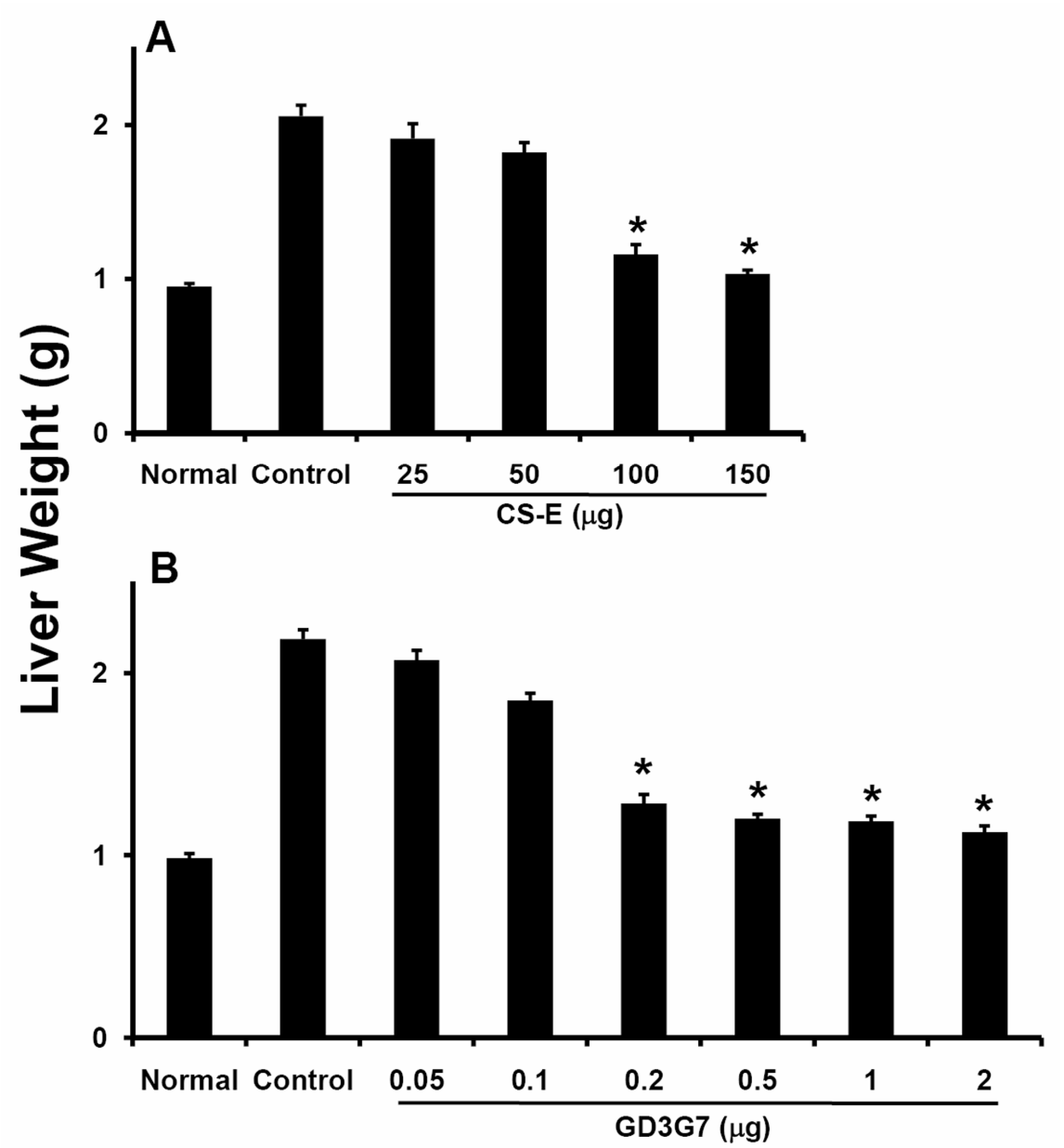
A
Liver Weight (g)
2
1
0
Normal Control
25
50
100
150
CS-E (μg)
B
2
1
0
Normal Control
0.05
0.1
0.2
0.5
1
2
GD3G7 (μg)

Fig 5

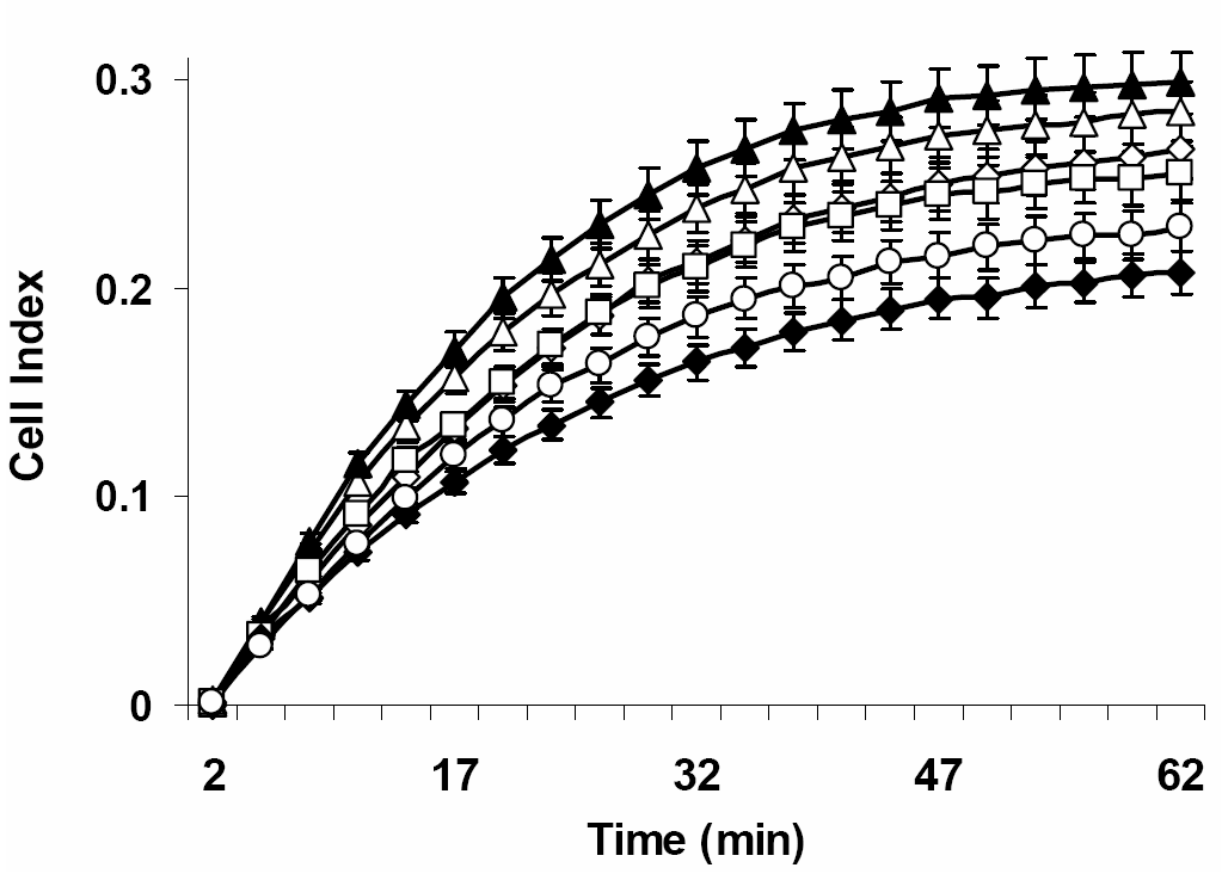

Fig 6

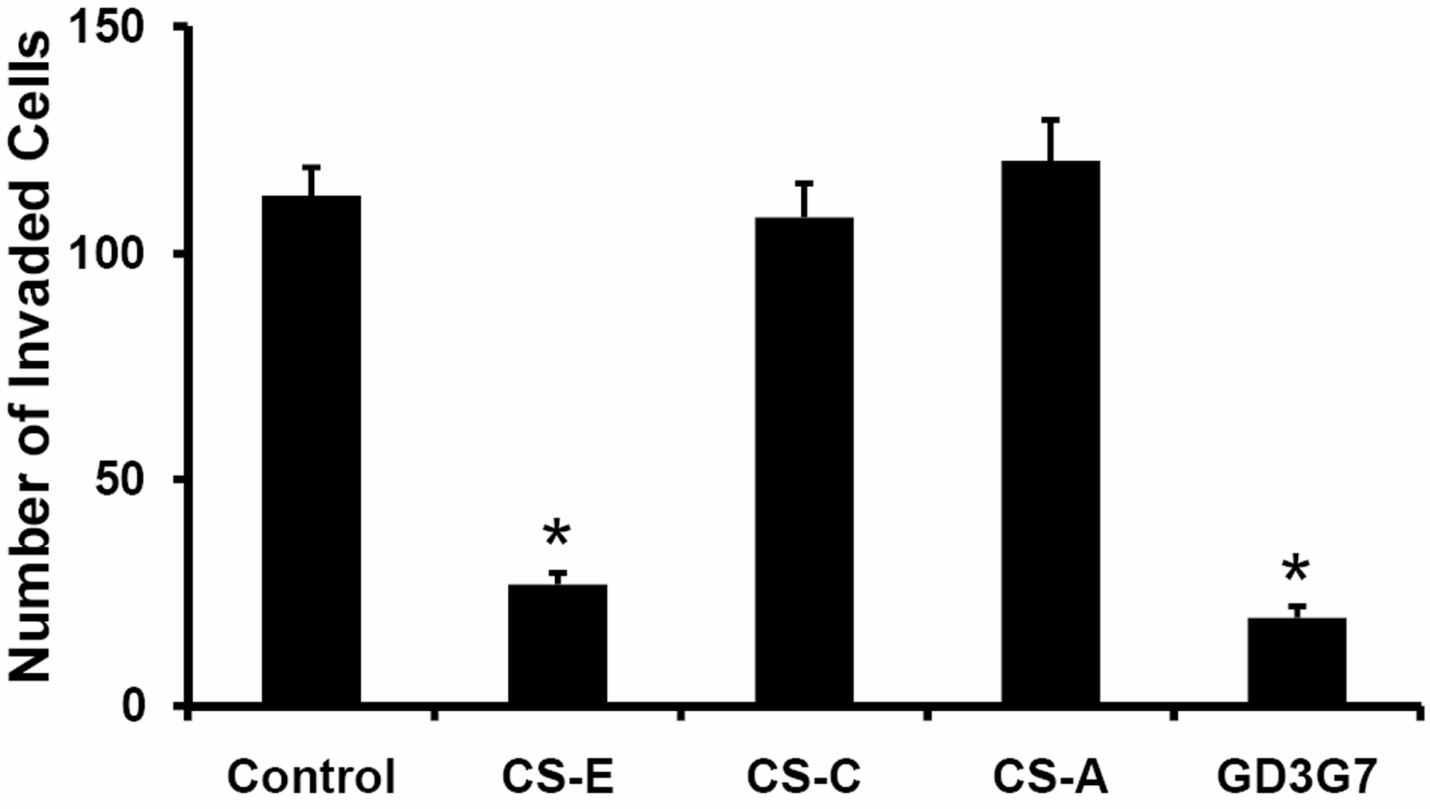
Number of Invaded Cells
150
100
50
0
*
*
Control
CS-E
CS-C
CS-A
GD3G7

Fig 7

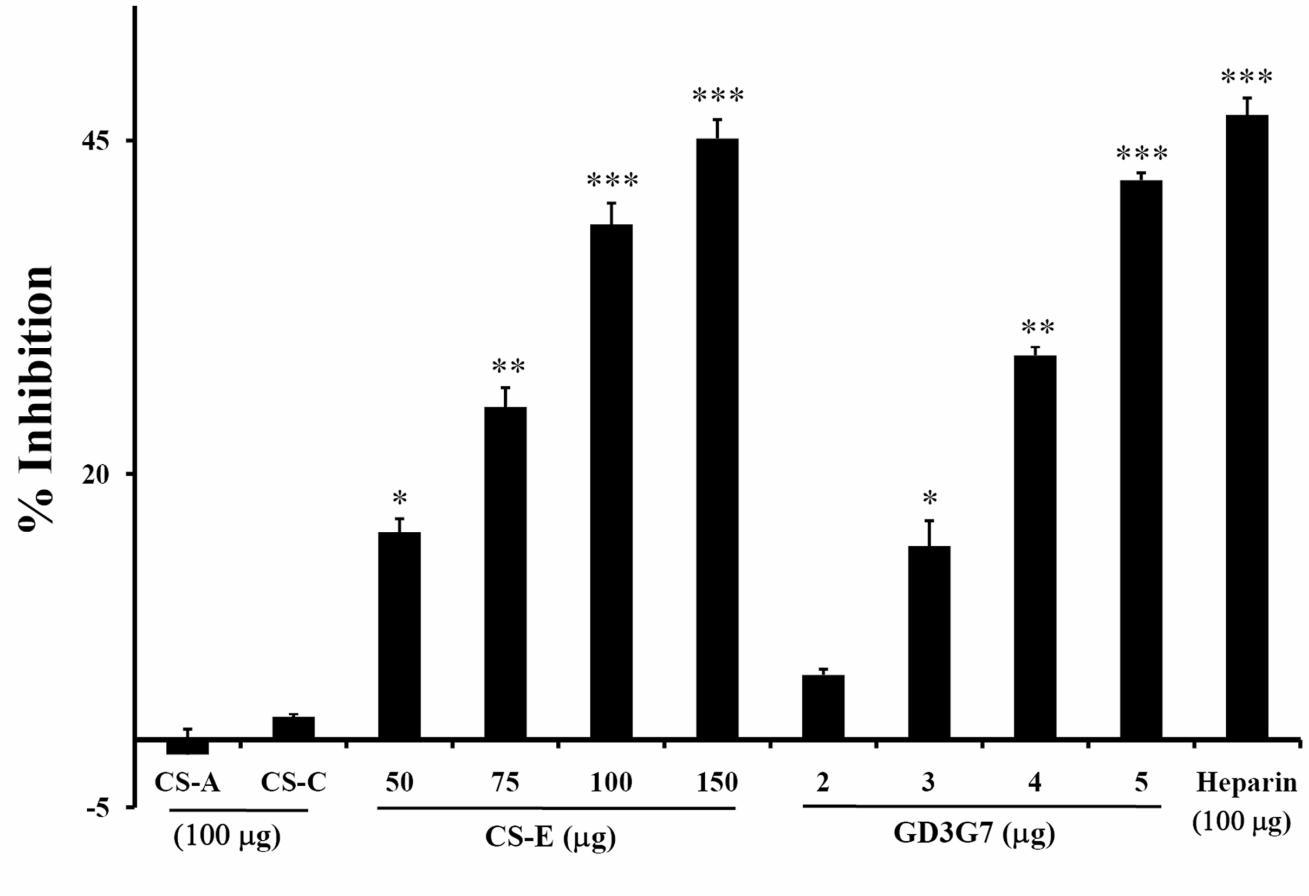
% Inhibition
45
20
-5
*
**
***
***
*
**
***
***
CS-A
CS-C
50
75
100
150
2
3
4
5
Heparin
(100 μg)
CS-E (μg)
GD3G7 (μg)
(100 μg)

Fig 8

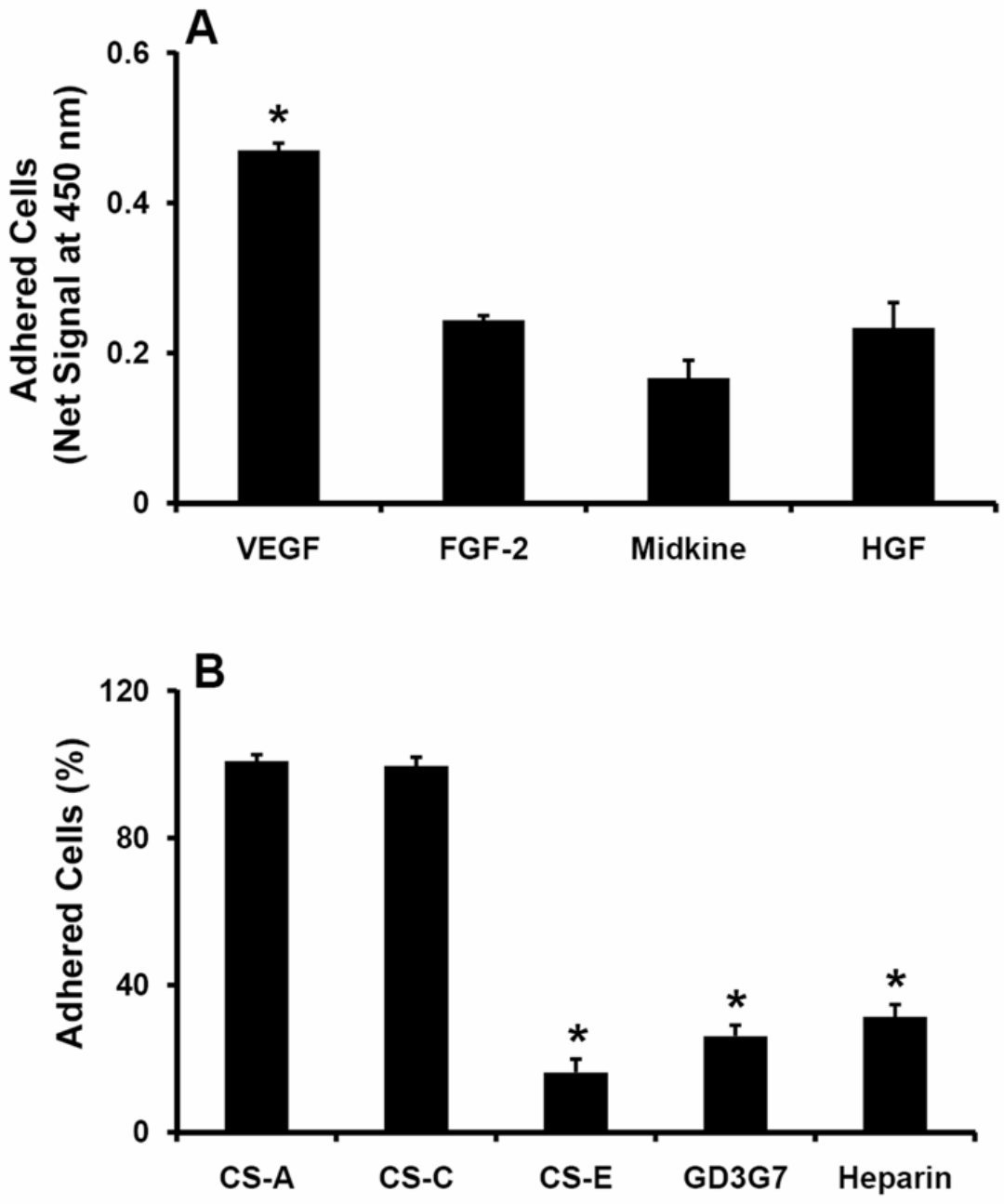
A
Adhered Cells
(Net Signal at 450 nm)
0.6
0.4
0.2
0
*
VEGF
FGF-2
Midkine
HGF
B
Adhered Cells (%)
120
80
40
0
*
*
*
CS-A
CS-C
CS-E
GD3G7
Heparin